

## Intrinsic modulation of pulse-coupled integrate-and-fire neurons

S. Coombes

*Nonlinear and Complex Systems Group, Department of Mathematical Sciences, Loughborough University,  
Leicestershire LE11 3TU, United Kingdom*

G. J. Lord

*Applied Nonlinear Mathematics Group, Department of Engineering Mathematics, Bristol University, University Walk,  
Bristol BS8 1TR, United Kingdom*

(Received 2 May 1997; revised manuscript received 8 July 1997)

Intrinsic neuromodulation is observed in sensory and neuromuscular circuits and in biological central pattern generators. We model a simple neuronal circuit with a system of two pulse-coupled integrate-and-fire neurons and explore the parameter regimes for periodic firing behavior. The inclusion of biologically realistic features shows that the speed and onset of neuronal response plays a crucial role in determining the firing phase for periodic rhythms. We explore the neurophysiological function of distributed delays arising from both the synaptic transmission process and dendritic structure as well as discrete delays associated with axonal communication delays. Bifurcation and stability diagrams are constructed with a mixture of simple analysis, numerical continuation and the Kuramoto phase-reduction technique. Moreover, we show that, for asynchronous behavior, the strength of electrical synapses can control the firing rate of the system.

[S1063-651X(97)14410-5]

PACS number(s): 87.10.+e, 02.30.Ks, 47.20.Ky

### I. INTRODUCTION

There are two sources of modulation for neuronal circuits: extrinsic, such as an external input, and intrinsic, such as variation of cell membrane properties. Intrinsic modulation is thought to produce local changes in neuronal computation in contrast to extrinsic modulation that can cause global changes [1]. This is well illustrated with the example of the neuronal circuits found in the crustacean stomatogastric ganglion [2]. Altering cellular and synaptic properties of neurons in this circuit causes different dynamical network behavior and hence the generation of distinct gastric rhythms [3]. Circuits that, by virtue of their intrinsic properties and synaptic interactions, generate and control the activity of motor neurons are called central pattern generators (CPGs). Intrinsic neuromodulation has been experimentally demonstrated in several biological CPGs [1,4,5], where a diverse repertoire of rhythmic motor behavior is possible in the absence of sensory feedback. It is believed that a brief initial stimulus triggers the intrinsic neuromodulation that arises from neurons within the CPG circuit allowing the production of a prolonged rhythmic pattern. For example, in the mollusc *Tritonia* [1] and the tadpole *Xenopus* [4] the escape swim behavior is generated in this fashion.

The study of coupled oscillators has applications in understanding CPG neuronal circuits such as those mentioned above. Indeed, systems of coupled nonlinear oscillators have recently attracted much interest in neurobiology due to the discovery of synchronized oscillations in the cat visual cortex [6]. Much of the theoretical work in this area uses the phase-coupled oscillator formalism developed by Kuramoto [7]. Moreover, there is also considerable interest in studying the dynamics of pulse-coupled neuronal models in which the details of individual spikes are included (see [8] for a review). The analysis of reciprocally connected neurons has

implications for understanding the mechanisms whereby rhythm generation (periodic behavior) is produced by a CPG in the absence of endogenous pacemaking cells. Reduced versions of the Hodgkin-Huxley equations including details of ionic currents have been studied numerically [9–13] while the analysis of coupled relaxation oscillators has allowed a more analytic approach [14]. We are careful to distinguish three forms of oscillations: a synchronous state, where neurons oscillate in phase, an antisynchronous state, where neurons oscillate in antiphase, and an asynchronous state, a state between the other two where neurons oscillate at an intermediate phase. In theoretical studies of pulse-coupled neuronal networks with fast synaptic responses, synchronization is typically obtained with excitatory connections between neurons [15–17]. However, neuronal CPGs and cortical tissue can maintain synchronous, antisynchronous, and asynchronous behavior. For example, the CPG for swimming in the tadpole *Xenopus* maintains an antiphase oscillatory rhythm to generate waves of bending along the spinal cord. Inhibitory synaptic connections undoubtedly play an important role in preventing large-scale synchronization. However, recent work suggests that other intrinsic mechanisms may also lead to desynchronization. Van Vreeswijk *et al.* [18] have shown that pulse-coupled integrate-and-fire neurons can desynchronize if the postsynaptic currents are sufficiently slow. Hence, distributed delays from synaptic transmission processes can effect the synchrony of simple coupled neural oscillators. This effect is also observed when more detailed single neuron models such as Hodgkin-Huxley are studied in the limit of weak coupling with the phase reduction technique of Kuramoto [18,19]. Also, Sherman and Rinzel [20] have shown numerically that strong electrical coupling leads to synchronous behavior for a pair of coupled neurons, but that weak electrical coupling can lead to antiphase oscillations. Similar observations have previously been made by

Mulloney *et al.* [21]. A more detailed analysis of this phenomenon was undertaken by Han *et al.* [22] using a combination of numerical simulation and the weak coupling phase reduction technique. They show that global electrical coupling leads to bursting behavior as well as the previously observed desynchronization. The neuronal propagation delays present in a system of interacting neurons are also thought to provide a mechanism for desynchronization. For the case of two pulse-coupled oscillators incorporating small delays, a return-map analysis [23,24], which generalizes the seminal work of Mirollo and Strogatz [15], reinforces this idea. Furthermore, in the presence of signal delays, the phase-coupled oscillator model of Kuramoto possesses multiple synchronous solutions [25] for two neurons and exhibits extremely rich asynchronous behavior for a population that interacts via time-delayed nearest-neighbor coupling [26]. The Kuramoto phase reduction technique has also recently been used to analyze the effects of axonal propagation delays [27] and dendritic structure on neuronal synchronization [28–30]. For neurons with no extended structure, propagation delays are solely dependent upon neuronal separation while neurons that filter synaptic input through a passive dendritic tree have responses that depend upon the distributed delays arising from the diffusion of a signal along the tree and the spatial location of the synapse.

In this paper we investigate sources of intrinsic neuromodulation for a simple model CPG. We consider a circuit of two identical integrate-and-fire neurons mutually coupled by identical excitatory synapses. The classification of dynamical behavior in different parameter regimes can be used to model the effects of intrinsic neuromodulation provided that the model maintains contact with biological reality. We focus on features of the single neuron that affect the neuronal response to synaptic stimulation. Since these in turn contribute to the nature of a network oscillation we are able to isolate the role that various cellular and synaptic properties have in determining circuit function. Importantly, in contrast to work discussed above and extending an earlier paper [31], we show that the competition between various neuronal length and time scales has important consequences for neurophysiological function. For example, the distributed delay that arises from the synaptic transmission process may result in a slow neuronal response, which in turn stabilizes an asynchronous network rhythm. However, the inclusion of a further delay, arising from say a finite axonal propagation velocity, can lead to a stable synchronous rhythm. Variation of the period of oscillation, as well as the phase, is also important in many biological CPGs. Electrical synapses between neurons are suggested as a possible source for the modulation of the firing period.

In detail, we take single spikes or *action potentials* as basic entities, communicated via chemical synapses. Presynaptic action potentials are considered to induce postsynaptic currents. These are described with functional forms that closely approximate real synaptic currents. Furthermore, we include transmission delays that model the finite axonal propagation time for action potentials. An integrate-and-fire model with linear cell membrane properties is essentially solvable using the variation-of-parameters formula. In Sec. II this approach is used to study the dynamics of the cell body (soma) of two such pulse-coupled neurons. In biological

CPGs with small neuronal populations, gap junctions or electrical synapses contribute significantly to network activity. The above model is extended to include bidirectional electrical synapses and reexpressed such that cell membrane potentials evolve according to a linear Volterra integrodifferential equation. Once again the variation-of-parameters formula is used in Sec. III to formulate solutions. Finally, in Sec. IV, we consider the effects of dendrites on phase synchronization by idealizing the dendritic tree as a semi-infinite one-dimensional structure described by a second-order linear partial differential equation, namely, the cable equation [32]. Assuming that the neurons intrinsically oscillate, a completely analytic discussion of the effects of the spatial location of the synaptic input is possible using the phase reduction technique of Kuramoto [7]. Results are exact for weak synaptic coupling and the case when the somatic feedback current from the soma to the dendrites is negligible. The stability of solutions is shown to depend upon both the natural frequency of oscillation and the point of synaptic contact.

Throughout the paper detailed numerical analysis, using AUTO94 [33], is used to explore the solution spaces generated using the variation-of-parameters formula. In essence, motivated by biological CPGs with intrinsic neuromodulation, we explore the role that variation of propagation time delays, rise and fall time of postsynaptic current pulses, strength of chemical and electrical coupling, and dendritic structure can have on the phase of periodic firing patterns for two pulse-coupled integrate-and-fire neurons. The consequences of this work for larger arrays are discussed in Sec. V.

## II. PULSATILE COUPLING WITH DELAYS IN AN INTEGRATE-AND-FIRE MODEL

We begin by considering two identical integrate-and-fire neurons with mutual excitatory coupling. Each neuron is regarded as a point processor with no extended dendritic structure. The state variable  $\phi_i(t)$ ,  $i=1,2$ , is used to represent the cell membrane potential at neuron 1 and 2, respectively. The neurons are assumed to fire whenever  $\phi_i(t)$  reaches some threshold  $h$ , after which  $\phi_i(t)$  is reset to some resting level, taken as zero (see Fig. 1). Denoting the time at which neuron  $i$  fires for the  $n$ th occasion  $T_n^i$ , since the initial firing time  $T_0^i$ , the potentials  $\phi_i(t)$  evolve according to the linear ordinary differential equations (ODEs)

$$\frac{d\phi_i}{dt} = -\frac{\phi_i}{\tau} + I_i(t), \quad t \in (T_k^i, T_{k+1}^i), \quad k \in \mathbb{Z} \quad (1)$$

with the strongly nonlinear reset conditions

$$\lim_{\epsilon \rightarrow 0_+} \phi_i(T_k^i - \epsilon) = h, \quad \lim_{\epsilon \rightarrow 0_+} \phi_i(T_k^i + \epsilon) = 0. \quad (2)$$

Here,  $I_i(t)$  represents the input to neuron  $i$  from neuron  $j$ , which is therefore dependent upon the firing history of the system. Equation (1) is simply the differential equation of an  $RC$  circuit of cell membrane resistance  $R$ , capacitance  $C$ , and hence, membrane time constant  $\tau=RC$ . Between firing events the unique solution to Eq. (1) is given using the variation-of-parameters formula,

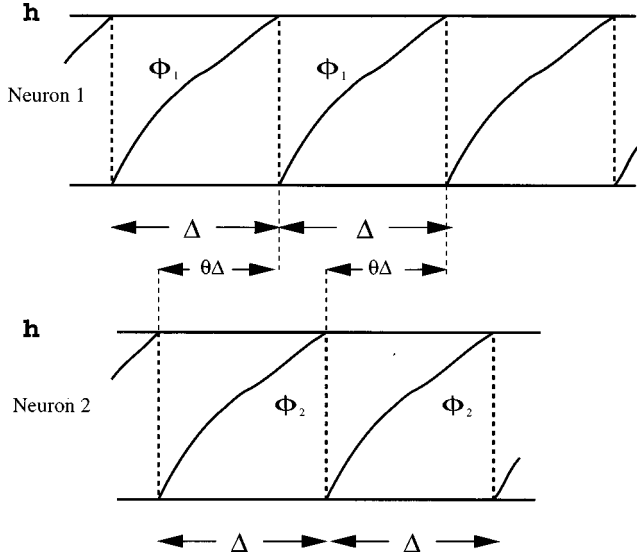


FIG. 1. Schematic diagram of the periodic solution for two pulse-coupled integrate-and-fire neurons with threshold  $h$ , period  $\Delta$ , and relative phase  $\theta$ .

$$\phi_i(t) = \int_{T_k^i}^t e^{-(t-t')/\tau} I_i(t') dt', \quad t \in (T_k^i, T_{k+1}^i). \quad (3)$$

The current  $I_i(t)$  should reflect the fact that postsynaptic currents are generated by the firing events or *spikes* of the presynaptic neuron  $j$ . These spikes are often modeled as simple Dirac  $\delta$ -function pulses [15,17,34]. However, the effective input to the postsynaptic neuron has a longer temporal duration due to the synaptic transmission process. One particular pulse shape that approximates the rise and fall time of real synaptic currents is the so-called  $\alpha$  function [35]. The consequences of the temporal duration of synaptic conductance changes within integrate-and-fire models has been discussed (for the case of  $\alpha$  functions) by several authors [18,36,37]. One should also be careful to incorporate delays due to finite axonal propagation times into the total synaptic current. With this in mind, we write the input to neuron  $i$  from neuron  $j$  as a sum of delayed  $\alpha$  functions such that

$$I_i(t) = \sum_{n \geq 1} P(t - T_n^j - t_d) \Theta(t - T_n^j - t_d), \quad j \neq i, \quad (4)$$

where  $t_d$  represents the axonal propagation delay time and  $P(t)$  takes the form of an  $\alpha$  function:

$$P(t) = g \alpha^2 t e^{-\alpha t}. \quad (5)$$

The strength of interaction is measured with the parameter  $g$ , while the exponential rise (and fall) rate of the synapse is equal to  $\alpha$ , such that the maximal synaptic response occurs at a time  $\alpha^{-1}$  after the arrival of an action potential. The step function  $\Theta(x)$  in Eq. (4) is equal to 1 for  $x > 0$  and vanishes for  $x \leq 0$ . In the steady periodic firing state defined by  $\lim_{k \rightarrow \infty} T_{k+1}^i - T_k^i \equiv \Delta$  (independent of initial conditions), the infinite sum in Eq. (4) can be reduced to a convergent geometric progression. In fact the input to neuron 2 (assuming that neuron 1 last fired at  $t=0$ ) takes the form  $I_2(t) = I_1(t)$ , where

$$I(t) = \frac{g \alpha^2 e^{-\alpha(t-t_d)}}{(1 - e^{-\alpha \Delta})} \left\{ (t - t_d) + \frac{\Delta e^{-\alpha \Delta}}{(1 - e^{-\alpha \Delta})} \right\}, \quad t \in [t_d, t_d + \Delta). \quad (6)$$

We now introduce a phase  $\theta$ ,  $0 \leq \theta \leq 1$ , such that if neuron 1 fires at  $t = T_k^1$  then neuron 2 fires at  $T_k^2 = T_k^1 - \theta \Delta$ , again at  $T_{k+1}^2 = T_k^1 + \Delta(1 - \theta)$ . This periodic behavior is illustrated in Fig. 1. In this case  $I_1(t) = I_2(t + \theta \Delta)$  and outside their ranges the  $I_i(t)$  are periodic:

$$I_1(t + n\Delta) = I_1(t), \quad t \in [t_d - \theta \Delta, t_d + \Delta(1 - \theta)), \quad (7)$$

$$I_2(t + n\Delta) = I_2(t), \quad t \in [t_d, t_d + \Delta), \quad n \in \mathbb{Z}. \quad (8)$$

To find the phase  $\theta$  and period  $\Delta$  for steady state periodic behavior we consider the simultaneous equations

$$\phi_1(\Delta) = h, \quad \phi_2(\Delta - \theta \Delta) = h. \quad (9)$$

For the membrane potentials  $\phi_i(t)$ ,  $i = 1, 2$ , given by Eq. (3) and  $I_i(t)$  given by Eq. (4), we may explicitly perform the integration in Eq. (9) and hence reduce Eq. (9) to a coupled system of algebraic equations. A simple condition on the phase and period is formed from the expression  $G(\theta, \Delta) = \phi_1(\Delta) - \phi_2(\Delta - \theta \Delta) = 0$ , where

$$G(\theta, \Delta) = e^{-\Delta/\tau} \int_0^\Delta dt' e^{t'/\tau} [I(t' + \theta \Delta) - I(t' - \theta \Delta)]. \quad (10)$$

Two obvious phase solutions, from the periodic properties of  $I(t)$ , are the synchronized solution with  $\theta = 0$  (or equivalently  $\theta = 1$ ) and the antisynchronous solution  $\theta = 1/2$ . Moreover, if  $\theta$  is a solution, then  $(1 - \theta)$  is also a solution. By manipulating the expression for  $G(\theta, \Delta)$  it is possible to form the relation  $\phi_2(\Delta - \theta \Delta) = h - G(\theta, \Delta)$ . Suppose  $\theta$  is slightly larger than a stable equilibrium value. Then neuron 2 should fire later to restore the correct value of  $\theta$ . This requires that  $\phi_2(\Delta - \theta \Delta)$  should be smaller than  $h$  or equivalently that  $G(\theta, \Delta)$  should be an increasing function of  $\theta$  near the equilibrium value. Otherwise a reset will occur, causing a dramatic change in the network dynamics. Hence, the condition for stability of a solution is defined by

$$\frac{\partial G(\theta, \Delta)}{\partial \theta} > 0. \quad (11)$$

All numerical results are produced using the continuation and bifurcation software AUTO94 [33]. Although primarily written for ODEs, AUTO94 can compute solution branches for algebraic systems of the form (9), detect simple bifurcation points, and compute bifurcating branches. Note that if Eq. (9) cannot be reduced explicitly to an algebraic system then a numerical quadrature method (such as composite Simpson's rule) may be applied to approximate the algebraic system. The stability of the branches may be established by evaluating the inequality (11).

In the numerical results that follow we have chosen a time scale such that  $\tau = 1$  and the constants  $g$  and  $h$  are fixed with  $g = 0.4$ ,  $h = 0.25$ . Pseudoarclength continuation was performed in either  $\alpha$  (with fixed  $t_d$ ) or  $t_d$  (with fixed  $\alpha$ ), solv-

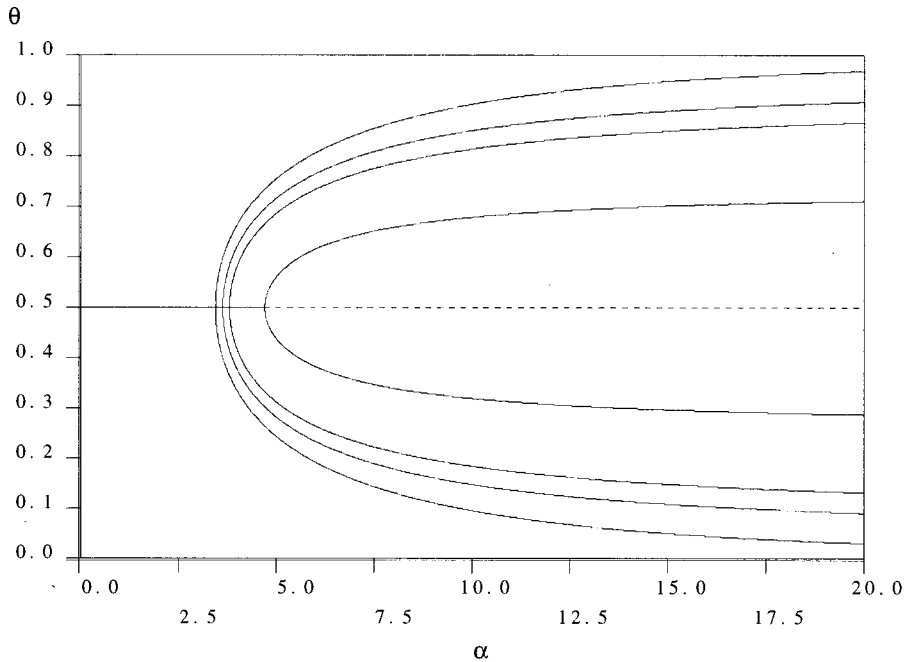


FIG. 2.  $\theta$  vs  $\alpha$  bifurcation diagram with  $\tau=1$  for varying delay times. The four branches above and below the antisynchronous state ( $\theta=1/2$ ) correspond to four differing values of the time delay  $t_d$ . The branch bifurcating from  $\theta=1/2$  at the lowest value of  $\alpha$  corresponds to the case with no delay,  $t_d=0$ . Successive bifurcations for progressively larger  $\alpha$  correspond to the case with delays,  $t_d=0.025$ ,  $t_d=0.05$ , and  $t_d=0.25$ , respectively. Solid (dashed) lines represent stable (unstable) solutions.

ing for the phase difference  $\theta$  and period  $\Delta$  in either case. It should be noted that on some of the branches in Figs. 2–5 bifurcations in  $\Delta$  were also found, for given values of  $\theta$ .

In Fig. 2 we plot the bifurcation diagram for the phase  $\theta$  versus  $\alpha$  in the presence of small delays and also for  $t_d=0$  (reproducing the results of Van Vreeswijk *et al.* [18]). For small values of the synaptic rate constant  $\alpha$  there are two possible states showing either complete synchrony,  $\theta=0,1$ , or complete antisynchrony,  $\theta=1/2$ . Only the antisynchronous state is stable. With increasing  $\alpha$ , corresponding to progressively faster synapses, there is a pitchfork bifurcation at a critical value of  $\alpha=\alpha^c$  and two additional equilibria are born. The antisynchronous solution loses stability and continues as an unstable branch. The two new states are stable and have intermediate phases, i.e., are neither synchronous nor antisynchronous and are referred to as asynchronous. As  $\alpha\rightarrow\infty$  the  $\alpha$  function approximates a Dirac  $\delta$  pulse and the stable asynchronous solutions approach closely to the perfectly synchronized solution (at  $\theta=0$  or  $\theta=1$ ). For small delays ( $t_d\leq 0.25$ ), once again there is a pitchfork bifurcation from a stable antisynchronous solution leading to the creation of two new stable states for some critical  $\alpha$ . An increase in  $t_d$  causes further desynchronization in the sense that the critical value for  $\alpha$  increases and for a fixed  $\alpha>\alpha^c$  the solution branches move inward toward the antisynchronous solution. In Figs. 3, 4, and 5 we show bifurcation diagrams for  $\theta$  versus  $t_d$  with several different  $\alpha$  values. Figure 3, with  $\alpha=3<\alpha^c$  (for  $t_d=0$ ), shows that for small  $t_d$  the antisynchronous solution is the only stable one. Increasing  $t_d$  leads to the creation of two new unstable branches, which eventually coexist with the synchronous solution. This phenomenon of bifurcation and approach to the synchronous solution is repeated at larger values of  $t_d$  but with an interchange of solution stabilities. For a fixed phase  $\theta$ , this leads to an alternating sequence of stable and unstable solutions with increasing  $t_d$ . In Fig. 4 we show behavior in the phase  $\theta$  as the delay  $t_d$  varies in the regime  $\alpha>\alpha^c$  (for  $t_d=0$ ). For small delays ( $t_d\leq 0.25$ ), Fig. 4, with  $\alpha=5$ , simply reex-

presses the results shown in Fig. 2 to the right of the largest value of  $\alpha^c$ . Note that as  $t_d$  is increased from zero the desynchronization effect becomes complete in the sense that the stable intermediate phase solutions join with the antisynchronous solution at  $t_d\sim 0.5$ . Beyond this point the antisynchronous solution becomes stable. Furthermore, two new stable solutions are born that approach the synchronous state with a further increase in  $t_d$ . A host of other solutions are born with increasing  $t_d$ . Moreover, the possibility exists for multiple synchronous and antisynchronous solutions to exist with differing periods and stabilities. Note that for  $\alpha\leq 5.85$  (Figs. 2, 3, 4) AUTO94 detected the bifurcations along the  $\theta=1/2$  branch, whereas for  $\alpha>5.9$  no bifurcations were detected following this branch. However, the bifurcating branches persist for  $\alpha>5.9$ , as is evident from Fig. 5. This

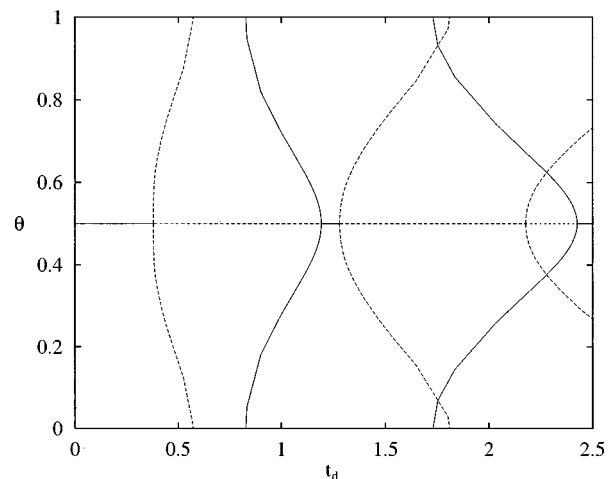


FIG. 3.  $\theta$  vs  $t_d$  bifurcation diagram for  $\alpha=3$ . Stable branches are denoted by solid lines and unstable branches by dashed lines. Regions where stable and unstable branches coexist are denoted with dotted lines. Note the existence of multiple solutions with a fixed value of the phase difference  $\theta$  and the checkerboard pattern of stable-unstable branches.

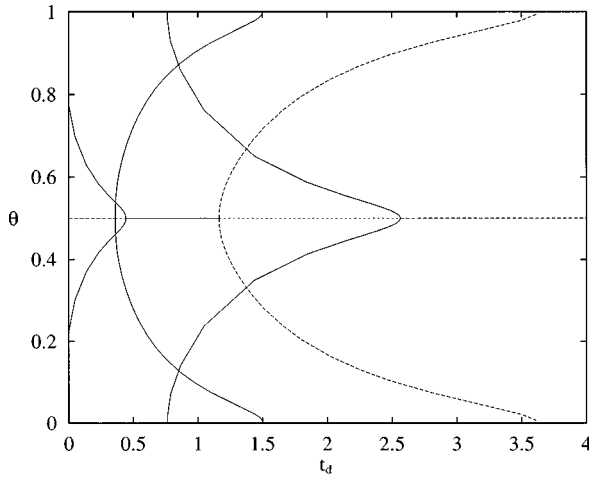


FIG. 4.  $\theta$  vs  $t_d$  bifurcation diagram for  $\alpha=5$ . Labeling for stability is the same as in Fig. 3.

figure was formed by continuing points on the branches in Fig. 4 in  $\alpha$  up to  $\alpha=10$  and then continuing each branch in the time delay  $t_d$ .

Recently Ernst *et al.* [23] and Mather and Mattfeldt [24] have analyzed the effect of propagation delays, in a similar system to that considered, communicating via strict Dirac  $\delta$  pulses. For excitatory couplings both conclude that for  $t_d < \Delta/2$  two new stable phase solutions are possible, supporting the idea that propagation delays can induce desynchronization. By taking a sufficiently large value of  $\alpha$  it is possible to make an interesting comparison with this work. In Fig. 5 we explore the *pulsed* regime by setting  $\alpha=10$  and construct the  $\theta$  vs  $t_d$  bifurcation diagram for  $\theta \geq 1/2$  (solutions with  $\theta < 1/2$  are easily generated by symmetry). For small  $t_d$  the synchronous solution ( $\theta=0,1$ ) is stable while the antisynchronous ( $\theta=1/2$ ) one is unstable. With increasing  $t_d$  the antisynchronous solution remains unstable, while an initially stable synchronous solution desynchronizes with increasing  $t_d$ . At  $t_d \approx \Delta/2$ , ( $t_d \approx 0.31$ ), a stable solution is born from  $\theta=1/2$ , which eventually approaches the synchronous state with a further increase in  $t_d$ . Furthermore, as be-

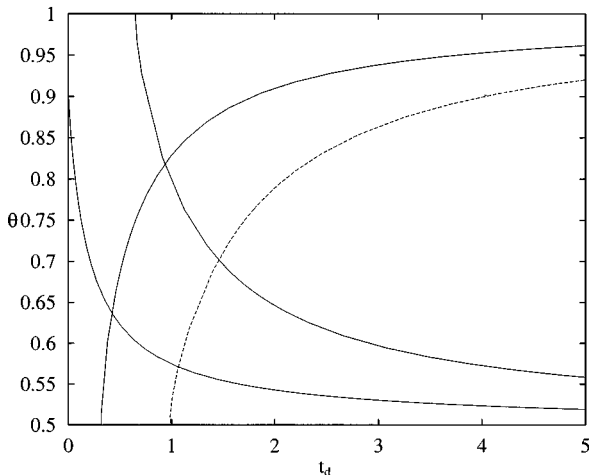


FIG. 5.  $\theta$  vs  $t_d$  bifurcation diagram for  $\alpha=10$  (fast synaptic response). Labeling for stability is the same as in Fig. 3. Note that solutions with  $\theta < 1/2$  may be generated by symmetry.

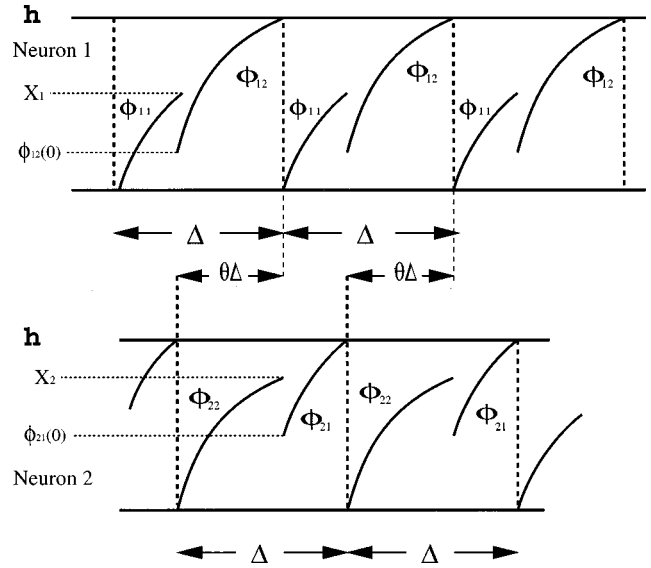


FIG. 6. Schematic diagram of the periodic solution for two pulse-coupled integrate-and-fire neurons with electrical coupling. The effect of reset is communicated between the two neurons via the direct electrical coupling and causes the discontinuous evolution of somatic potentials over a firing interval  $\Delta$ .

fore, other solutions are created with increasing  $t_d$ . In fact in this pulsed regime ( $\alpha \rightarrow \infty$ ) with  $t_d < \Delta/2$  our results are in agreement with those of Ernst *et al.* and Mather and Mattfeldt [24]. However, in the regime where their analysis does not apply ( $t_d \geq \Delta/2$ ) we see the creation of new solutions and multiple mixed stability synchronous and antisynchronous solutions. For very large  $t_d$  all solutions approach either the synchronous or antisynchronous states, both of which possess stable solutions for some period  $\Delta$ . Note that multistable dynamical systems have important applications as pattern recognition and memory storage devices. Indeed, the conditions under which time-delayed recurrent loops of integrate-and-fire neurons exhibit multistability has recently been investigated [38].

### III. ELECTRICAL AND CHEMICAL COUPLING

In addition to chemical synapses, there are many examples of direct electrical connections between cells. These connections occur via channels that span the presynaptic and postsynaptic membranes and are called *gap junctions*. Electrical synapses are present in many invertebrate nervous systems such as the gastric CPG of the previously mentioned crab. For CPGs found in invertebrates with small numbers of neurons it is common to find reciprocal inhibition between bursting neurons in conjunction with electrical coupling. Interestingly, electrical synapses have recently been found in a simple vertebrate, namely, between motor neurons in the spinal cord of the *Xenopus* tadpole [39]. Hence, dynamics of coupled neuronal oscillators including direct electrical connections may have a role in determining the functional significance of gap junctions.

As before we consider the evolution of the membrane potential  $\phi_i(t)$ ,  $i=1,2$ , for two identical pulse-coupled integrate-and-fire neurons, firing periodically (of period  $\Delta$ ). We now incorporate the effects of a bidirectional gap junc-

tion. To describe the dynamics (illustrated in Fig. 6), it is convenient to introduce the following notation:

$$\phi_i(t+T^j) = \phi_{ij}(t), \quad t \in (0, \tilde{\Delta}_j), \quad i, j = 1, 2, \quad (12)$$

where  $T^j$  denotes the time that neuron  $j$  last fired,  $\tilde{\Delta}_1 = \Delta(1 - \theta)$  and  $\tilde{\Delta}_2 = \theta\Delta$ . The total period  $\Delta = \tilde{\Delta}_1 + \tilde{\Delta}_2$ . The reset conditions, (2), become

$$\lim_{\epsilon \rightarrow 0_+} \phi_i(T^i + \epsilon) = \phi_{ii}(0) = 0, \quad i = 1, 2 \quad (13)$$

$$\lim_{\epsilon \rightarrow 0_+} \phi_i(T^i - \epsilon) = \phi_{ij}(\tilde{\Delta}_j) = h, \quad i, j = 1, 2, \quad i \neq j. \quad (14)$$

From Kirchoff's law the cell membrane potentials evolve according to

$$\frac{d\phi_{ij}}{dt} = -\frac{\phi_{ij}}{\tau} + \sigma(\phi_{i\bar{j}} - \phi_{ij}) + I_i(t + \eta_i\theta\Delta), \quad t \in (0, \tilde{\Delta}_j), \quad (15)$$

with  $\bar{i} = 1$  if  $i = 2$  and vice versa,  $\eta_1 = 0$  and  $\eta_2 = -1$ . The parameter  $\sigma = 1/(rC)$  incorporates the resistance  $r$  of the electrical synapse between the two neurons and reflects the strength of electrical coupling. Note that the effect of reset is communicated between neurons due to this coupling and gives rise to the discontinuous evolution of cell membrane potentials over a whole period  $\Delta$  (as shown in Fig. 6). For simplicity we drop all discussion of discrete time delays and set  $t_d = 0$ . However, their effects may be incorporated with the method used in Secs. II and III if one so wishes. Once again the variation-of-parameters formula may be used to write a solution as

$$\begin{aligned} \phi_i(t) = & e^{-\epsilon t} \phi_{ij}(0) + \int_0^t e^{-\epsilon(t-t')} [I_i(t' + \eta_i\theta\Delta) \\ & + \sigma \phi_{i\bar{j}}(t')] dt', \quad t \in (0, \tilde{\Delta}_j), \end{aligned} \quad (16)$$

where  $\epsilon = \tau^{-1} + \sigma$ . Hence, by substitution of Eq. (16) into Eq. (15), we may form the integro-differential equation

$$\frac{d\phi_{ij}}{dt} = -\epsilon \phi_{ij} + \int_0^t H(t-t') \phi_{ij}(t') dt' + F_{ij}(t), \quad (17)$$

where  $H(t) = \sigma^2 e^{-\epsilon t}$  and

$$\begin{aligned} F_{ij}(t) = & I_i(t + \eta_j\theta\Delta) + \sigma e^{-\epsilon t} \phi_{i\bar{j}}(0) \\ & + \sigma \int_0^t e^{-\epsilon(t-t')} I_{i\bar{j}}(t' + \eta_j\theta\Delta) dt'. \end{aligned} \quad (18)$$

Thus, between resets, the  $\phi_{ij}(t)$  evolve according to a linear Volterra integral-differential equation. Each neuron behaves like the original integrate-and-fire neuron of Sec. II, but with an external input  $F_{ij}(t)$  [instead of just  $I_i(t)$ ] and an additional feedback contribution that takes into account electrical coupling via the gap junction. The feedback transfer function is  $H(t)$ . A unique solution of the model may be constructed that generalizes that of Sec. II. Since both the convolution kernel  $H(t)$  and the function  $F_{ij}(t)$  are continuous on  $(0, \tilde{\Delta}_j)$

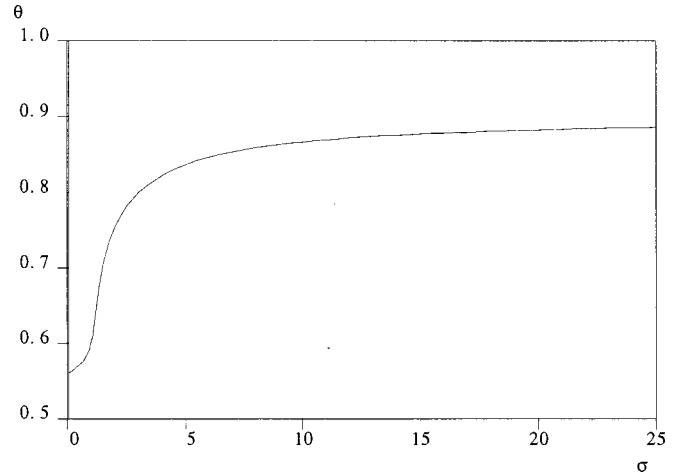


FIG. 7. Variation of phase  $\theta$  in a network with both electrical and chemical coupling as a function of the strength of electrical interaction.  $\alpha = 5.5$ ,  $X_1 = 6.58 \times 10^{-2}$ ,  $X_2 = 9.94 \times 10^{-2}$ ,  $\phi_{12}(0) = 1.28 \times 10^{-3}$ , and  $\phi_{21}(0) = 4.08 \times 10^{-2}$ .

we can apply the following result due to Burton [40]. If  $Z(t)$  is the solution of the homogeneous equation

$$\frac{dZ}{dt} = -\epsilon Z + \int_0^t H(t-t') Z(t') dt', \quad Z(0) = 1 \quad (19)$$

and if  $\phi_{ij}(t)$  is a solution of Eq. (17) on  $(0, \tilde{\Delta}_j)$  then

$$\phi_{ij}(t) = Z(t) \phi_{ij}(0) + \int_0^t Z(t-t') F_{ij}(t') dt'. \quad (20)$$

Hence,  $\phi_{ij}(t)$  is uniquely determined by the initial condition  $\phi_{ij}(0)$  together with a variation of parameters solution (20). With the use of Laplace transforms and the Bromwich theorem, Eq. (19) may be solved as

$$Z(t) = \frac{1}{2} (e^{\epsilon_+ t} + e^{\epsilon_- t}), \quad (21)$$

where  $\epsilon_{\pm} = \epsilon \pm \sigma$ . We may now self-consistently solve the equations for the somatic potentials to determine both the phase  $\theta$  and period  $\Delta$  in the steady state. Simultaneously solving  $\phi_{11}(\Delta(1 - \theta)) = X_1$ ,  $\phi_{22}(\theta\Delta) = X_2$ ,  $\phi_{12}(\theta\Delta) = h$  and  $\phi_{21}(\Delta(1 - \theta)) = h$ , yields the unknowns  $\theta$ ,  $\Delta$ ,  $\phi_{12}(0)$ , and  $\phi_{21}(0)$ , where  $X_{1,2}$  must be determined self-consistently with  $X_{1,2} < h$ . Numerically we apply numerical quadrature to reduce these equations to an algebraic system. As before, we construct the function  $G(\theta, \Delta)$  as

$$G(\theta, \Delta) = \phi_{12}(\theta\Delta) - \phi_{21}(\Delta(1 - \theta)) = 0. \quad (22)$$

The condition for stability is  $\partial G(\theta, \Delta) / \partial \theta > 0$ . Note that in the limit of no electrical coupling  $\sigma \rightarrow 0$  we recover the solutions for the somatic potentials given in Sec. II.

In Fig. 7 we plot the variation of relative phase  $\theta$  as a function of the strength of electrical interaction  $\sigma$  for a restricted set of parameters, namely,  $\alpha = 5.5$ ,  $X_1 = 6.58 \times 10^{-2}$ ,  $X_2 = 9.94 \times 10^{-2}$ ,  $\phi_{12}(0) = 1.28 \times 10^{-3}$ , and  $\phi_{21}(0) = 4.08 \times 10^{-2}$  with all remaining parameters as in Sec. II. It appears from numerical experiments that new solutions cannot be created but rather that weak coupling can favor nearly antisynchronous phase relationships, while

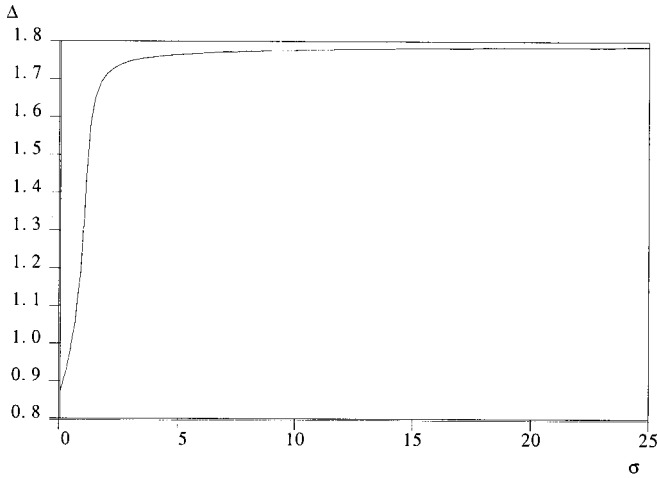


FIG. 8. Variation of period  $\Delta$  for the system defined in Fig. 7, highlighting the functional significance of the strength of electrical coupling in modulating system firing frequency.

strong electrical coupling can increase the synchrony of solutions. More interesting is the observation that small changes in the strength of electrical coupling can lead to sharp changes in the period of oscillation. This can be seen in Fig. 8 for the corresponding plot of Fig. 7 for variation of the period  $\Delta$  with  $\sigma$ . Such an effect has also been observed for asynchronous periodic rhythms generated in a similar system of two chaotic neurons [41]. From a functional point of view the mixture of electrical and chemical coupling provides a high sensitivity for period regulation of the asynchronous periodic state.

#### IV. EFFECTS OF DENDRITIC STRUCTURE

In general, the diffusive nature of dendrites means that the single neuron somatic response is a convolution of the synaptic input with the response function of the dendritic tree. Furthermore, the precise ordering of the axonal fiber system in cortical regions suggest that the synaptic locations of inputs play a role in circuit function [42]. Rospars and Lansky [43] have described the response of a compartmental model in which it is assumed that dendritic potentials evolve without any influence from the nerve impulse generation process. However, the electrical coupling between the soma and dendrites means that there is a feedback signal across the dendrites whenever the somatic potential resets. This situation is described in detail by Bressloff [44]. The basic idea is to eliminate the passive component of the dynamics (the dendritic potential) to yield a Volterra integrodifferential equation for the somatic potential. An iterative solution to the integral equation can be constructed in terms of a second order map of the firing time, in contrast to a first order map as found in models lacking dendritic structure [45]. Unfortunately, a description of two pulse-coupled compartmental models with reset is analytical unwieldy, although some work on this problem has been done by Crook [28]. However, substantial progress can be made by considering the dendritic tree of a neuron to be idealized as a semi-infinite one-dimensional cable [32]. Furthermore, it is illuminating to work in the *phase*-interaction representation, rather than the *pulse*-interaction picture used until now. This can be

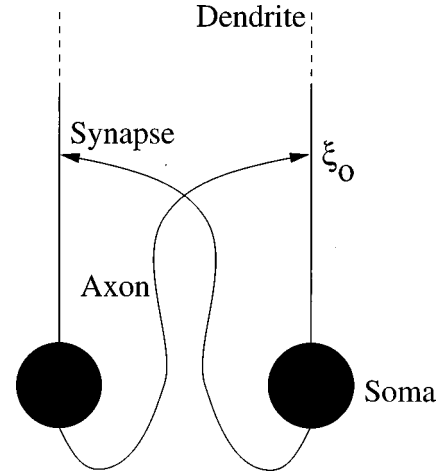


FIG. 9. Interaction schematic for two pulse-coupled integrate-and-fire neurons with idealized dendritic structure. Synaptic input occurs at synapses located a distance  $\xi_0$  from the soma.

achieved using the formalism developed by Kuramoto and others [7,18] and, in this particular instance, helps to isolate the contribution of dendritic structure to neuronal synchronization. We show that the synchronous solution can change from stable to unstable as the point of synaptic input moves further from the soma (see Fig. 9). Independent work by Crook [28] on cells connected by synapses at the ends of finite dendritic cables (with variable space constant) reinforces these results. Both Crook [28] and Bressloff and Coombes [29] propose that this mechanism may be used by neural circuits, whereby proximal connections encourage synchrony and more distal encourage asynchrony or antisynchrony.

In general, cell membrane properties are such that there is a nonlinear relationship between membrane ionic current and the transmembrane potential [35,46]. In fact a more realistic scenario than so far considered is given by the equations (for  $i=1,2$ )

$$\frac{\partial V_i(\xi, t)}{\partial t} = D \frac{\partial^2 V_i(\xi, t)}{\partial \xi^2} - \frac{V_i}{\tilde{\tau}} + E_i(\xi, t), \quad (23)$$

$$\frac{d\phi_i}{dt} = f(\phi_i) + \rho_0[V_i(0, t) - \phi_i(t)], \quad 0 < \phi_i(t) < h. \quad (24)$$

Equation (23) is the standard cable equation for the dendritic potential  $V_i(\xi, t)$  of an unbranched dendrite on neuron  $i$ , with dendritic coordinate  $\xi \in \mathbb{R}^+$ . The decay constant  $\tilde{\tau}$  and the diffusion constant  $D$  may be related to underlying cellular properties of dendritic tissue and in the following analysis we fix length and time scales by setting  $D = \tilde{\tau} = 1$ . The soma is considered to be sited at position  $\xi = 0$  on the cable and  $\mathcal{I}_i(t) = \rho_0[V_i(0, t) - \phi_i(t)]$  is the current density flowing to the soma from the cable. The equation for the dendritic potential  $V_i(\xi, t)$  has input  $E_i(\xi, t)$  representing the synaptic input, taken to be absent at the soma. Equation (23) is supplemented by the boundary condition  $-\partial V_i / \partial \xi|_{\xi=0} = \mathcal{I}_i(t)$ . Equation (24) (without the  $\rho_0$ -dependent coupling term) for the somatic potential  $\phi_i(t)$  of a neuron was originally proposed by Abbott and Kepler [47] through a system-

atic reduction of the Hodgkin-Huxley equations. Furthermore, they have shown using experimental data that  $f(\phi)$  can be fitted with a cubic [47]. In order to simplify our analysis, we shall assume that the current flowing from the soma to the dendrite is negligible, which amounts to imposing the homogeneous boundary condition  $\partial V_i / \partial \xi|_{\xi=0} = 0$ . After absorbing a term  $-\rho_0 \phi_i$  into the definition of the function  $f(\phi_i)$  in Eq. (24) we have that  $\mathcal{I}_i(t)$  is transformed to  $\rho_0 V_i(0, t)$ . We now solve Eq. (23) for  $V_i(\xi, t)$  in terms of the synaptic inputs and set  $\xi=0$  to give

$$\mathcal{I}_i(t) = 2\rho_0 \int_{-\infty}^t dt' \int_0^{\infty} d\xi' K(\xi', t-t') E_i(\xi', t'), \quad (25)$$

where  $K(\xi, t) = e^{-t - \xi^2/4t} / \sqrt{4\pi t}$  is the response or Green's function of the infinite cable equation. For concreteness we consider synaptic input on the cable to impinge at location  $\xi_0$  only such that

$$E_i(\xi, t) = \delta(\xi - \xi_0) I_i(t) \quad (26)$$

where  $I_i(t)$  has the form of Eq. (4).

The analytical intractability of this model is much reduced with the aid of averaging techniques valid in the limit of weak coupling. Indeed a nonlinear transform may be used to study nonlinear integrate-and-fire neurons in the framework of *pulse-coupled phase models* [8]. In the uncoupled state each identical neuron is imagined to fire with a natural period  $\Delta$  at times  $-\theta_i \Delta$ . Weak coupling of the two neurons will induce some relative phase relationship. The dynamical variable of interest in the weak-coupling regime is the phase of each oscillator. Specifically, following [18] one can apply the following nonlinear transform to Eq. (24):

$$\theta_i(t) + \frac{t}{\Delta} = \psi(\phi_i(t)) \equiv \frac{1}{\Delta} \int_0^{\phi_i(t)} \frac{d\phi'}{f(\phi')}, \quad (27)$$

with  $\Delta = \int_0^h d\phi' / f(\phi')$ . The phase variables  $\theta_i$  satisfy

$$\frac{d\theta_i}{dt} = J(t/\Delta + \theta_i) \mathcal{I}_i(t), \quad t \in (-\theta_i \Delta, (-\theta_i + 1)\Delta), \quad (28)$$

where  $J(z) = \Delta^{-1} / [f \circ \psi^{-1}(z)]$ , and  $J(z+n) = J(z)$ ,  $n \in \mathbb{Z}$ . Neuron  $i$  fires when  $\phi_i = h$  or equivalently, from Eq. (27), when  $\theta_i + t/\Delta = n$  for integer  $n$ . The corresponding firing times are  $t = (n - \theta_i)\Delta$  and hence

$$I_i(t) = I(t + \theta_i \Delta), \quad t \in [-\theta_i \Delta, (-\theta_i + 1)\Delta), \quad (29)$$

where  $I(t)$  is given by Eq. (6) and  $I(t+n\Delta) = I(t)$ . However, to simplify matters further still we shall drop discussion of transmission delays by setting  $t_d = 0$  and ignore the shape of postsynaptic currents so that  $I(t) = g \sum_n \delta(t - n\Delta)$ . Now assume that the term  $t/\Delta$  varies much more quickly than either of the  $\theta_i(t)$ , which is true for weak coupling. Then we can average the right side of Eq. (28) over one period  $\Delta$  and substitute Eqs. (25), (26), and (29) to obtain

$$\frac{d\theta_i}{dt} = \mathcal{H}(\theta_j - \theta_i), \quad (30)$$

with

$$\mathcal{H}(\theta) = g \int_0^{\infty} dt J(t - \theta) K(\xi_0, t\Delta) \quad (31)$$

and we have absorbed the factor of  $2\rho_0$  within the coupling strength  $g$ . As discussed in [18], the function  $J(t)$  is the phase interaction function of the model in the case of an instantaneous synapse. The function  $\mathcal{H}(\theta)$  involves the convolution of the instantaneous interaction function  $J(t)$  with the dendritic response function  $K(\xi_0, t)$ , which depends explicitly on the location  $\xi_0$  of the synapse on the dendritic cable. It follows that  $\mathcal{H}(\theta)$  can be written as a function of the phase difference,  $\theta = \theta_1 - \theta_2$ , by invoking the periodicity properties of  $J(t)$  and  $I(t)$ . The evolution of the phase difference may now be written as

$$\frac{d\theta}{dt} = -\mathcal{G}(\theta), \quad \mathcal{G}(\theta) = \mathcal{H}(\theta) - \mathcal{H}(-\theta). \quad (32)$$

Solutions can be found by solving Eq. (32) for  $\theta$  in the steady state,  $\mathcal{G}(\theta) = 0$ , with  $\Delta$  given by Eq. (27). Solutions are stable if  $\partial \mathcal{G}(\theta) / \partial \theta > 0$ . Since  $\mathcal{H}(\theta)$  is periodic with period 1,  $\mathcal{G}(\theta)$  always has zeros at  $\theta = 0, 1/2, 1$ . For simplicity, we shall take  $J(t) = -\sin 2\pi t$ , which is known to be a good approximation when  $f$  of Eq. (24) has an experimentally determined form [19]. Using the following Fourier representation of the fundamental cable solution:  $K(\xi_0, t) = (2\pi)^{-1} \int_{-\infty}^{\infty} dk e^{ik\xi_0 - \epsilon(k)t}$ , where  $\epsilon(k) = k^2 + 1$ , the stability function  $\mathcal{G}(\theta)$  becomes

$$\mathcal{G}(\theta) = g \sin(2\pi\theta) \int_{-\infty}^{\infty} \frac{dk}{2\pi} e^{ik\xi_0} A(k) \quad (33)$$

with

$$A(k) = \frac{\epsilon(k)}{\epsilon(k)^2 + \omega^2}, \quad \omega = \frac{2\pi}{\Delta}. \quad (34)$$

Hence, stability is partly dependent upon whether  $\hat{A} = \int_{-\infty}^{\infty} dk e^{ik\xi_0} A(k) > 0$ . The integral  $\hat{A}$  can be evaluated by closing the contour in the upper-half complex  $k$  plane as

$$\hat{A} = \frac{\pi}{r} e^{-r\xi_0 \cos(\beta/2)} [r\xi_0 \sin(\beta/2) + \beta/2], \quad (35)$$

with  $r^2 = \sqrt{1 + \omega^2}$  and  $\tan \beta = \omega$ ,  $0 \leq \beta \leq \pi/2$ . We deduce from Fig. 10 that as the distance  $\xi_0$  of the synapse from the soma increases from zero,  $\hat{A}$  reaches a critical value where a change in solution stability can occur. Increasing  $\xi_0$  still further produces alternating bands of stability and instability for solutions to  $\mathcal{G}(\theta) = 0$ . In fact, the synchronous state ( $\theta = 0, 1$ ) is stable for  $\hat{A} > 0$  and the antisynchronous state ( $\theta = 1/2$ ) is



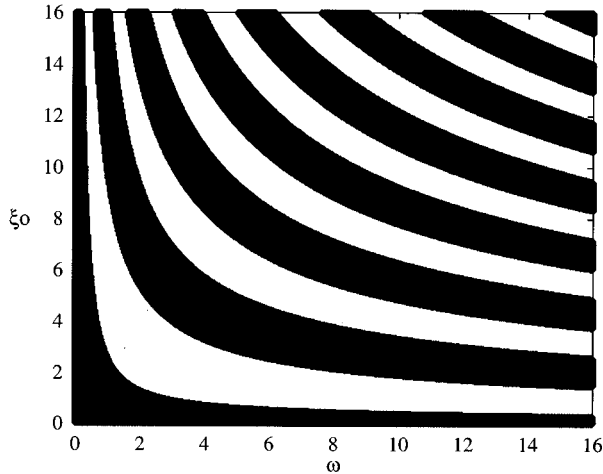


FIG. 10. Sign of  $\hat{A}$ ,  $\xi_0$  vs  $\omega$ . Black (white) regions correspond to  $\hat{A} > 0$  ( $\hat{A} < 0$ ). Note the checkerboard pattern of stability-instability, for say the synchronous solution, with increasing synaptic distance,  $\xi_0$ , for a fixed natural neuronal oscillator frequency  $\omega$ .

stable for  $\hat{A} < 0$  for excitatory coupling ( $g > 0$ ). A similar checkerboard structure of stable-unstable solutions with increasing axonal communication delay is seen in Figs. 3–5. Hence,  $\xi_0$  plays an analogous role to that of a time delay, since the time of maximal response at the soma due to an input at  $\xi_0$  increases with  $\xi_0$ . Interestingly this *time to peak* can be as large as a few hundred msec whereas axonal delays are typically 1–10 msec.

## V. DISCUSSION

The nonlinear dynamics of populations of pulse-coupled neuron models is of great importance in modeling the generation of biological rhythms. In general, neuronal pools can produce antisynchronous, asynchronous, as well as synchronous firing patterns. Hence, identifying the biological features that lead to such behaviors is important. In this paper we have focused on a very simple model of a central pattern generator (CPG) built from two pulse-coupled integrate-and-fire neurons. The inclusion of simple measures of axonal propagation delay, the pulse shape of postsynaptic currents, and electrical synapses can all be analyzed using elementary analysis in conjunction with numerical techniques for constructing bifurcation diagrams. The inclusion of a dendritic structure complicates such an approach, yet it is a vital component of most single-neuron anatomies. However, the spatiotemporal filtering properties of dendrites can be isolated with a reduction of the model, valid for intrinsically oscillating weakly coupled neurons. Moreover, such a reduced model is exactly solvable. By maintaining contact with neurophysiological reality both discrete and distributed delays arise naturally within the model CPG circuit description. Indeed, the rate of synaptic response (linked to the opening and closing of ion channels) allows the possibility of asynchronous periodic rhythms for sufficiently slow synapses [ $\alpha \sim O(1)$  with  $\tau = 1$ ], while the synchronous state is preferred for instantaneous synapses. Another form of distributed delay arises from the diffusive nature of a passive dendritic tree since the *time to peak* of a signal depends on the

distance of synaptic input from the soma. For some ranges of distance of the synapse from the soma the synchronous state can be destabilised in favor of an antisynchronous periodic rhythm. The more obvious delays inherent in many neuronal systems come in the form of communication delays. Not only can these discrete delays lead to stable asynchronous solutions for fast synaptic responses, but they allow the formation of multiple stable periodic orbits with the same phase but differing period. Hence, they are obviously important in the construction of memory devices [38]. An interesting issue arises concerning transitions between these attractors and will be addressed elsewhere. Moreover, delays of the above type have other important consequences in larger systems than those considered here. Interestingly, if the effective communication delay between neurons in a one-dimensional array of weakly coupled integrate-and-fire neurons is sufficiently large, then the synchronous state can be destabilized in favor of a state of stable traveling waves. This picture is valid when effective somatic responses are *fast* compared to the natural frequency of neuronal oscillation, but is altered in the presence of say slow synapses or dendritic structure as expected from the results presented here (see [30] for further discussion). The distributed and discrete delays arising naturally in neuronal systems may therefore be responsible for the oscillatory waves observed in such structures as the olfactory cortex where distributed delays arise from both synaptic and dendritic properties and discrete delays arise from the large axonal separations between neurons [28,29]. An important source of control of the period of the system resides in the strength of electrical connections between neurons. The combination of synaptic and gap junctions is typical for many small CPG circuits found in invertebrates. The sharp variation of period with small change in strength of electrical coupling is also observed by Huerta *et al.* [41], for the case of two coupled chaotic neurons, who suggest that the function of such a combination is to allow modulation of the period of asynchronous rhythms. Such a result highlights the importance of exploring the consequences of simple biological features in establishing rhythmic behavior in coupled neuronal systems, since useful conclusions can be drawn about neurophysiological function. Finally, let us make the point that many CPG circuits are of the *half-center* [48] variety, which rely upon reciprocal inhibition for rhythm generation rather than reciprocal excitation as considered here. In this case one requires extra physiological factors such as post-inhibitory rebound [49,50] or the inclusion of an external driving current for rhythm maintenance. In the case of a half-center oscillator with reciprocal inhibition and a sufficiently large external driving current (so that firing can occur in the absence of any coupling), bifurcation diagrams are qualitatively the same as those presented here, but with a reversal of stability for all solution branches.

## ACKNOWLEDGMENTS

The authors would like to thank Paul Bressloff and Bard Ermentrout for helpful comments during the completion of this work. Both authors are supported by the applied nonlinear mathematics initiative of the EPSRC (UK). S.C. was funded by Grant No. GR/K86220 and G.J.L. by Grant No. GR/J97199 of the EPSRC (UK).

- [1] P. S. Katz and W. N. Frost, *Trends Neurosci.* **19**, 54 (1996).
- [2] J. M. Weimann, P. Meyrand, and E. Marder, *J. Neurophysiol.* **65**, 111 (1991).
- [3] A. I. S. R. M. Harris-Warwick, E. Marder, and M. Moulins, *Dynamical Biological Networks: The Stomatogastric Nervous System* (MIT Press, Cambridge, MA 1992).
- [4] A. Roberts, *Science Progress Oxford* **74**, 31 (1990).
- [5] Y. I. Arshavsky *et al.*, *Trends Neurosci.* **16**, 227 (1993).
- [6] W. Singer, in *The Handbook of Brain Theory and Neural Networks*, edited by M. A. Arbib (MIT Press, Cambridge, MA 1995), pp. 960–963.
- [7] Y. Kuramoto, *Chemical Oscillations, Waves and Turbulence* (Springer-Verlag, New York, 1984).
- [8] W. Gerstner, *Phys. Rev. E* **51**, 738 (1995).
- [9] X. Wang and J. Rinzel, *Neural Comput.* **4**, 84 (1992).
- [10] F. K. Skinner, G. G. Turrigiano, and E. Marder, *Biol. Cybern.* **69**, 375 (1993).
- [11] F. K. Skinner, N. Kopell, and E. Marder, *J. Comput. Neurosci.* **1**, 69 (1994).
- [12] N. Kopell and G. LeMasson, *Proc. Natl. Acad. Sci. USA* **91**, 10 586 (1994).
- [13] T. LoFaro, N. Kopell, E. Marder, and S. L. Hooper, *Neural Comput.* **6**, 69 (1994).
- [14] N. Kopell and D. Somers, *J. Math. Biol.* **33**, 261 (1995).
- [15] R. E. Mirollo and S. H. Strogatz, *SIAM (Soc. Ind. Appl. Math.) J. Appl. Math.* **50**, 1645 (1990).
- [16] Y. Kuramoto, *Physica D* **50**, 15 (1991).
- [17] J. J. Hopfield and A. V. M. Herz, *Proc. Natl. Acad. Sci. USA* **92**, 6655 (1995).
- [18] C. van Vreeswijk, L. F. Abbott, and G. B. Ermentrout, *J. Comput. Neurosci.* **1**, 313 (1994).
- [19] D. Hansel, G. Mato, and C. Meunier, *Europhys. Lett.* **23**, 367 (1993).
- [20] A. Sherman and J. Rinzel, *Proc. Natl. Acad. Sci. USA* **89**, 2471 (1992).
- [21] B. Mulloney, D. H. Perkel, and R. W. Budelli, *Brain Res.* **229**, 25 (1981).
- [22] S. K. Han, C. Kurrer, and Y. Kuramoto, *Phys. Rev. Lett.* **75**, 3190 (1995).
- [23] U. Ernst, K. Pawelzik, and T. Geisel, *Phys. Rev. Lett.* **74**, 1570 (1995).
- [24] R. Mather and J. Mattfeldt, *SIAM (Soc. Ind. Appl. Math.) J. Appl. Math.* **56**, 1094 (1996).
- [25] H. G. Schuster and P. Wagner, *Prog. Theor. Phys.* **81**, 939 (1989).
- [26] E. Niebur, H. G. Schuster, and D. Kammen, *Phys. Rev. Lett.* **67**, 2753 (1991).
- [27] S. M. Crook, G. B. Ermentrout, M. C. Vanier, and J. M. Bower, *J. Comput. Neurosci.* **4**, 161 (1997).
- [28] S. M. Crook, Ph.D. thesis, University of Maryland, 1996.
- [29] P. C. Bressloff and S. Coombes, *Phys. Rev. Lett.* **78**, 4665 (1997).
- [30] P. C. Bressloff and S. Coombes, *Int. J. Mod. Phys. B* (to be published).
- [31] S. Coombes and G. J. Lord, *Phys. Rev. E* **53**, R2104 (1996).
- [32] W. Rall, in *Methods in neuronal Modelling*, edited by C. Koch and I. Segev (MIT Press, Cambridge, MA, 1992), Chap. 2, pp. 9–62.
- [33] E. Doedel, H. B. Keller, and J. P. Kernevez, *Int. J. Bif. Chaos* **1**, 493 (1991).
- [34] M. Tsoodyks, I. Mitkov, and H. Sompolinsky, *Phys. Rev. Lett.* **71**, 1280 (1993).
- [35] J. J. B. Jack, D. Noble, and R. W. Tsien, *Electric Current Flow in Excitable Cells* (Oxford Science Publications, New York, 1975).
- [36] L. F. Abbott and C. van Vreeswijk, *Phys. Rev. E* **48**, 1483 (1993).
- [37] W. Gerstner and J. L. van Hemmen, *Phys. Rev. Lett.* **71**, 312 (1993).
- [38] J. Foss, A. Longtin, B. Mensour, and J. Milton, *Phys. Rev. Lett.* **76**, 708 (1996).
- [39] R. Perrins and A. Roberts, *J. Neurophysiol.* **73**, 1005 (1995).
- [40] T. A. Burton, *SIAM Rev.* **25**, 343 (1983).
- [41] R. Huerta, M. I. Rabinovich, H. D. I. Abaranel, and M. Bazhenov, *Phys. Rev. E* **55**, R2108 (1997).
- [42] G. M. Shepherd, in *The Synaptic Organization of the Brain*, edited by G. M. Shepherd (Oxford University Press, New York, 1990), pp. 3–31.
- [43] J. P. Rospars and P. Lansky, *Biol. Cybern.* **69**, 283 (1993).
- [44] P. C. Bressloff, *Physica D* **80**, 399 (1995).
- [45] J. P. Keener, F. C. Hoppensteadt, and J. Rinzel, *SIAM (Soc. Ind. Appl. Math.) J. Appl. Math.* **41**, 503 (1981).
- [46] D. Johnston and S. M. Wu, *Foundations of Cellular Neurophysiology* (MIT Press, Cambridge, MA, 1995).
- [47] L. F. Abbott and T. B. Kepler, in *Statistical Mechanics of Neural Networks*, Lecture Notes in Physics Vol. 368, edited by L. Garrido (Springer-Verlag, Berlin, 1990).
- [48] R. L. Calabrese, in *The Handbook of Brain Theory and Neural Networks*, edited by M. A. Arbib (MIT Press, Cambridge, MA, 1995), pp. 444–447.
- [49] S. Coombes and S. H. Doole, *Dyn. Stability Syst.* **11**, 193 (1996).
- [50] S. Coombes and S. H. Doole, *Phys. Rev. E* **54**, 4054 (1996).